Spin-reorientation transitions and crystalline-electric-field parameters in $R\mathrm{Fe}_{10}T_2$ (R = rare earth; T = Si or V) intermetallic compounds

C. Christides, M. Anagnostou, Hong-Shuo Li,* A. Kostikas, and D. Niarchos
National Center for Scientific Research "Demokritos," Institute of Materials Science, 153 10 Aghia Paraskevi Attiki, Greece

(Received 11 December 1990; revised manuscript received 22 February 1991)

The spin-reorientation transition temperatures T_{SR} in some $R\mathrm{Fe}_{10}T_2$ intermetallic compounds (T=Si or V) have been determined from an analysis of the temperature dependence of the Mössbauer spectra and thermomagnetic measurements. These results were used for estimating the crystalline-electric-field coefficients A_{nm}. The preferential-site-occupation probabilities for a Si atom to occupy one of the available special positions 8i, 8j, and 8f in the $R\mathrm{Fe}_{10}\mathrm{Si}_2$ lattice have also been determined from the analysis of the Mössbauer spectra. A comparison of the A_{n0} obtained for the $R\mathrm{Fe}_{12-x}T_x$ compounds, with T=Ti, V, or Si, as a function of the preferential site occupation of the T atoms and of the T-atom concentration x reveals a decrease in A_{n0} with increasing T-atom occupation of the 8i site.

INTRODUCTION

The intrinsic magnetic properties of the pseudobinary alloys $R\mathrm{Fe}_{12-x}T_x$ (R=rare earth; T=Ti, V, Cr, Mo, W, or Si) have been the subject of several recent studies in view of their prospects as permanent magnet material alternatives to the Nd-Fe-B alloys. Although the results have shown that the expected performance cannot equal that of the Nd-Fe-B magnets, these studies have demonstrated that the 1:12 alloys offer several advantages for understanding magnetic exchange and crystal-field interactions in iron-rich rare-earth intermetallic alloys. First, because of the fact that the anisotropy of the iron sublattice is comparable to the second-order anisotropy from the rare-earth sublattice and greater than higher-order terms, a rich variety of magnetic structures is observed which can be used as a testing ground for theoretical models. Another significant advantage is that the rare-earth ion occupies only one crystallographic site of high symmetry (4/*mmm*), so that only five crystalline-electric-field (CEF) coefficients are required, compared to 18 for the $R_2\mathrm{Fe}_{14}\mathrm{B}$ compounds. The single-ion magnetic exchange and crystalline-electric-field interaction model, originally formulated for the explanation of the magnetic properties of the $R_2\mathrm{Fe}_{14}\mathrm{B}$ compounds,[1] has been applied with remarkable success also to the $R\mathrm{Fe}_{12-x}T_x$ alloys. A set of five (CEF) coefficients has been derived from magnetization measurements on a single crystal of $\mathrm{DyFe}_{11}\mathrm{Ti}$,[2] which were subsequently applied for the quantitative explanation of the observed spin-reorientation transitions (SRT) in the $R\mathrm{Fe}_{11}\mathrm{Ti}$ (Ref. 2) series.

A direct application of these parameters to the $R\mathrm{Fe}_{10}\mathrm{V}_2$ alloys has been used[3] in order to test the reliability of the obtained crystal-field coefficients A_{nm} to another 1:12 series. The explanation of the observed SRT in $\mathrm{HoFe}_{10}\mathrm{V}_2$ in contrast to the expected but not observed SRT in $\mathrm{HoFe}_{11}\mathrm{Ti}$ has been given in terms of a weakening of the Fe sublattice anisotropy due to the two V atoms, instead of one Ti atom, which are needed in order to stabilize the 1:12 phase. But the differences between the experimental and calculated SRT temperatures T_{SR}, especially for the compounds with R=Nd and Dy, are indicative that a modification of the A_{nm} is necessary for the V series. In both these series of alloys, the early transition metal occupies preferentially one of the three crystallographic sites occupied by iron, namely, the 8i site.[4,5] In the $R\mathrm{Fe}_{10}\mathrm{Si}_2$ series, on the other hand, the Si atoms occupy preferentially the 8j and 8f positions in the unit cell.[6] This fact, in combination with the metalloid character of Si, is expected to alter significantly the CEF coefficients.

In order to understand the effect of the preferential site occupation of T atoms on the crystal-field interactions, we examine in this work the SRT transitions of the $R\mathrm{Fe}_{10}\mathrm{Si}_2$ compounds using Mössbauer and magnetization data as a function of temperature for the calculation of the A_{nm} in this series. In addition, we fit again a new set of A_{nm} for the $R\mathrm{Fe}_{10}\mathrm{V}_2$ compounds which reproduce correctly all the observed SRT transitions and we compare all the above crystal-field coefficients with those obtained for the $R\mathrm{Fe}_{11}\mathrm{Ti}$ series as a function of the concentration x and preferential site occupation of T=Ti, V, and Si atoms in the three inequivalent iron sites 8i, 8j, and 8f.

EXPERIMENTAL RESULTS

The $R\mathrm{Fe}_{10}\mathrm{Si}_2$ alloys (R=Y, Tb, Dy, Ho, Er, or Tm) for this investigation were prepared by arc melting stoichiometric amounts of the constituents. Powder x-ray diagrams show that the ingots consist of a pure phase of the ThMn_{12}-type structure with small traces of α-Fe only in the $\mathrm{HoFe}_{10}\mathrm{Si}_2$ compound. It was found impossible to stabilize the compound with R=Nd in the 1:12-type structure. Oriented samples for Mössbauer and magnetization measurements were prepared by solidifying mixtures of the powder with epoxy resin in a magnetic field of 12 kG.

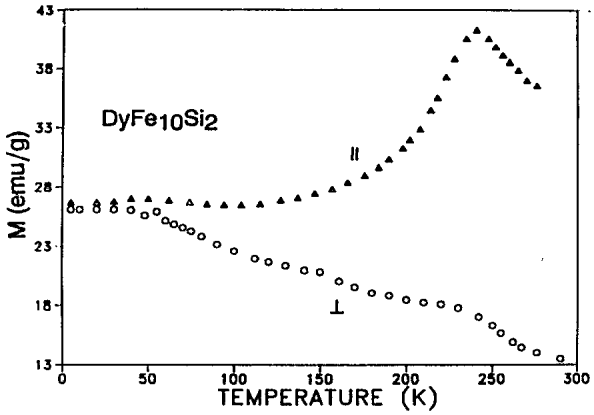

FIG. 1. Magnetic moments $M_{\parallel}$ and $M_{\perp}$ vs temperature for the $DyFe_{10}Si_2$ compound in an applied field of 500 G.

The temperature dependence of the magnetization was measured in a homogeneous field of 500 G in the temperature range of 4.2–300 K, following an isothermal measurement at 4.2 K, up to a field of 20 kG, by using a PAR-155 vibrating-sample magnetometer. The results for two different directions of the applied field, parallel ($M_{\parallel}$) and perpendicular ($M_{\perp}$) to the direction of orientation, are shown in Fig. 1 for the $DyFe_{10}Si_2$ compound and in Fig. 2 for the rest of the alloys. The deviation of the $M_{\parallel}$ and $M_{\perp}$ curves in opposite directions indicate the existence of SRT transitions for the alloys $DyFe_{10}Si_2$ and $TbFe_{10}Si_2$ only. High-temperature ($T > 300$ K) magnetic measurements of ingot samples have been performed by using a Perkin-Elmer thermogravimetric balance (TGA) in a high-purity argon atmosphere in a small inhomogeneous applied field. In Fig. 3 we present the magnetic curves with ascending and descending temperature, in the same applied field, for the $TbFe_{10}Si_2$ ingot. The abrupt decrease of the magnetization before reaching the Curie temperature T_C of the 1:12 phase in the heating-up curve, which is not observed in the curve with decreasing temperature, might be attributed to the occurrence of a first-order SRT transition.

For the compounds with R=Tb, Er, Ho, and Tm, ^{57}Fe Mössbauer spectra have been obtained with oriented absorbers at three temperatures T=5, 80, and 290 K and for R=Dy, measurements on an oriented absorber have been performed at 11 different temperatures in the T=5–290 K range. The direction of the γ rays in these measurements was parallel to the orientation axis.

The spectra were fitted by assuming three statistically independent probabilities p_i, p_j, and p_f for the average occupation of the 8i, 8j and 8f iron sites, respectively, by Si atoms. A binomial distribution of populations was used for each site, corresponding to different environments as described in previous studies.[7] The relative intensities of the lines of the magnetic sextet components were taken as $3{:}x{:}1{:}1{:}x{:}3$, where x is a parameter determined by the fitting procedure, depending on the tilting angle of the magnetic moment with respect to the c axis

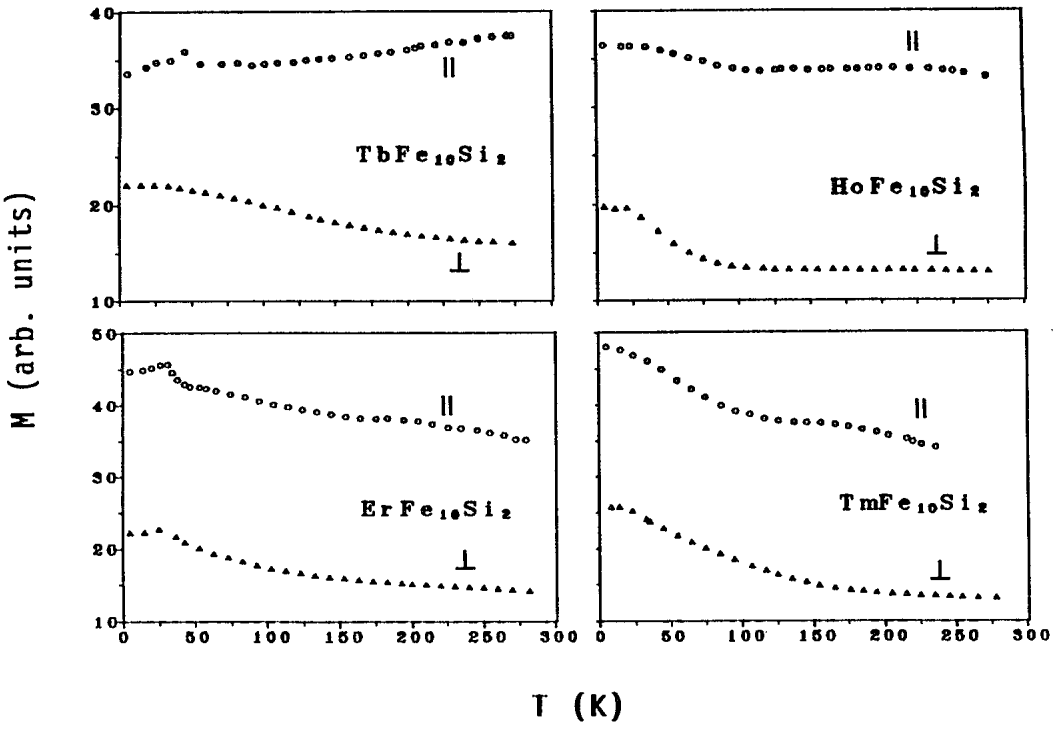

FIG. 2. Magnetic moments $M_{\parallel}$ and $M_{\perp}$ vs temperature for the $RFe_{10}Si_2$ compounds with R=Tb, Ho, Er, and Tm.

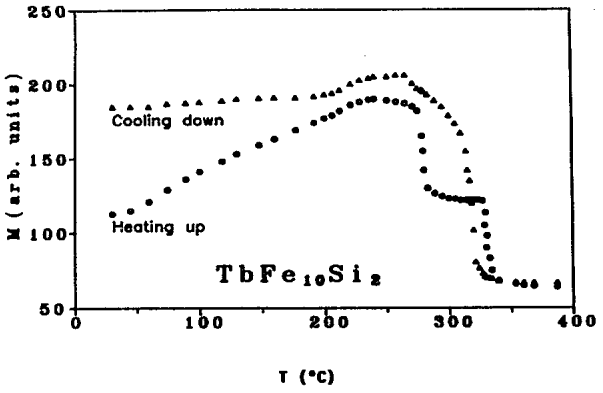

FIG. 3. High-temperature magnetic measurements performed with thermogravimetric analysis on a $TbFe_{10}Si_2$ ingot.

and the degree of orientation.

In Fig. 4 are plotted the fitted absorption spectra of $DyFe_{10}Si_2$ from the contribution of the three hyperfine-field-distribution subspectra, which correspond to each one of the three lattice sites 8i, 8j, and 8f. The spectra show clearly the decrease of the ratio I_2/I_1 of the intensities of the first two absorption lines, arising from the rotation of magnetization toward the c axis in the temperature range 200–280 K. The variation of the resulting hyperfine fields (B_{eff}) for each site 8i, 8j, and 8f as a function of temperature is shown in Fig. 5. A significant continuous decrease of the B_{eff} for the 8i site in the SRT temperature range is observed beyond that expected from the temperature dependence of magnetization.

In Figs. 6 and 7 we present the fitted absorption spectra of the $RFe_{10}Si_2$ compounds with R=Tb and Er, re-

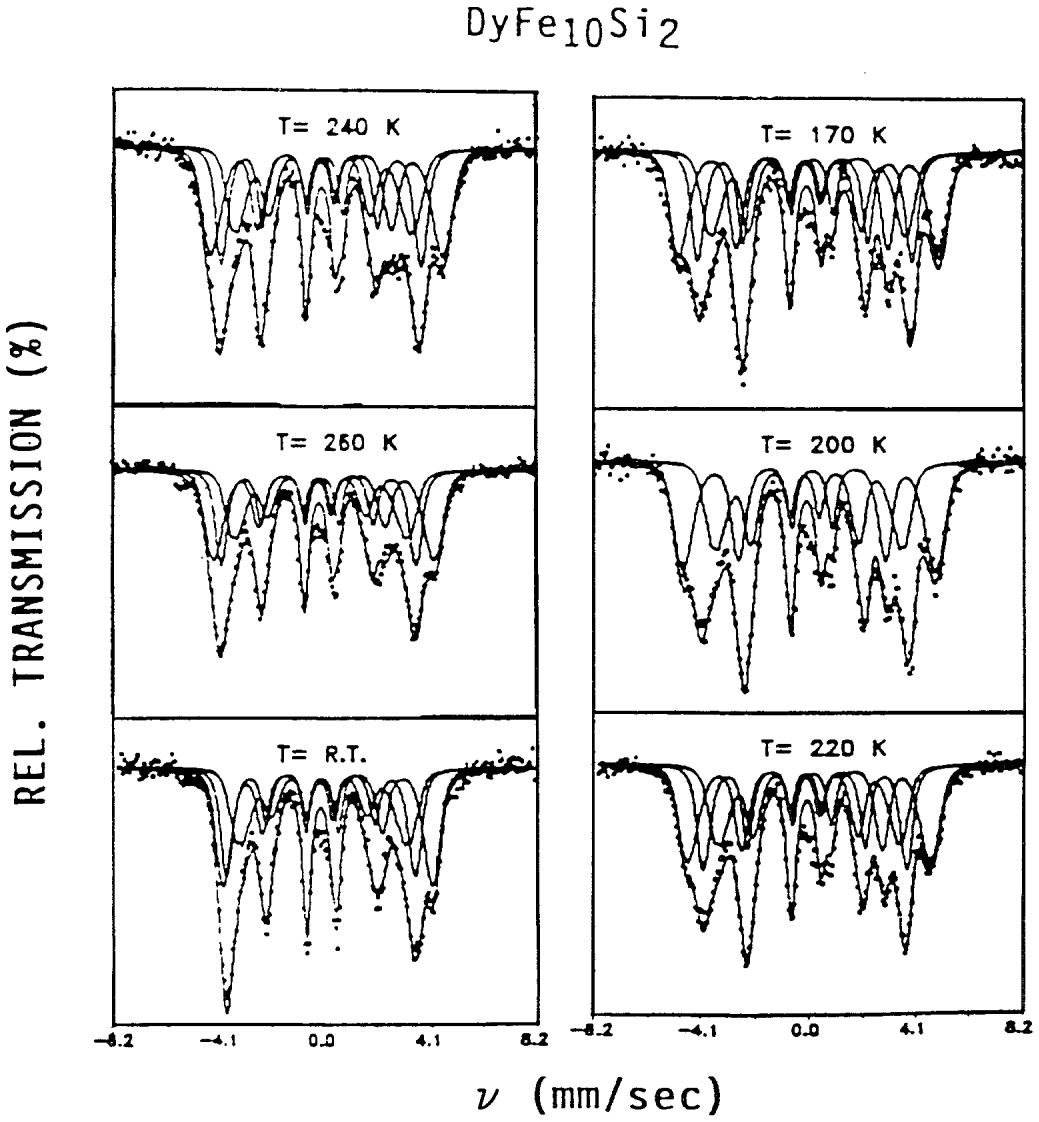

FIG. 4. Mössbauer spectra of $DyFe_{10}Si_2$ from oriented polycrystalline absorbers. The solid line is a least-squares fit with the model described in the text.

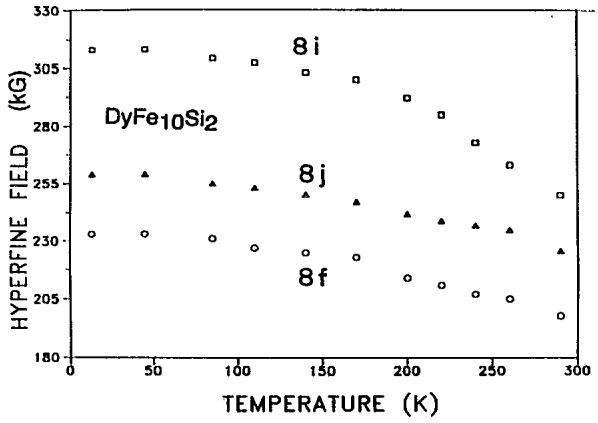

FIG. 5. Variation of H_{HF} for sites 8i, 8j, and 8f as a function of temperature for the compound $DyFe_{10}Si_2$.

spectively. The spectra for R=Ho and Tm at all temperatures present similar line-shape patterns with those of Er. They consist of narrow distributions of the hyperfine fields for each lattice site and the magnetic sextets of the 8i, 8f, and 8j sites correspond to similar hyperfine parameters B_{eff}, Δ_{IS}, and Δ_{QS} for these members of the series, as shown in Table I. From the magnetization measurements in Fig. 2 and the parameter x which measures the relative intensity of the $\Delta m = 0$ line (Table I), it is clear that there are no SRT transitions throughout the temperature range where these three compounds are magnetically ordered. The easy axis of magnetization is always parallel to the c axis. The fact that x is different from zero as expected for magnetic moments parallel to the γ-ray direction can be attributed to incomplete orientation of the crystallites in the sample, as discussed in detail in previous reports.[7] In support of this conclusion, we note also that for R =Dy

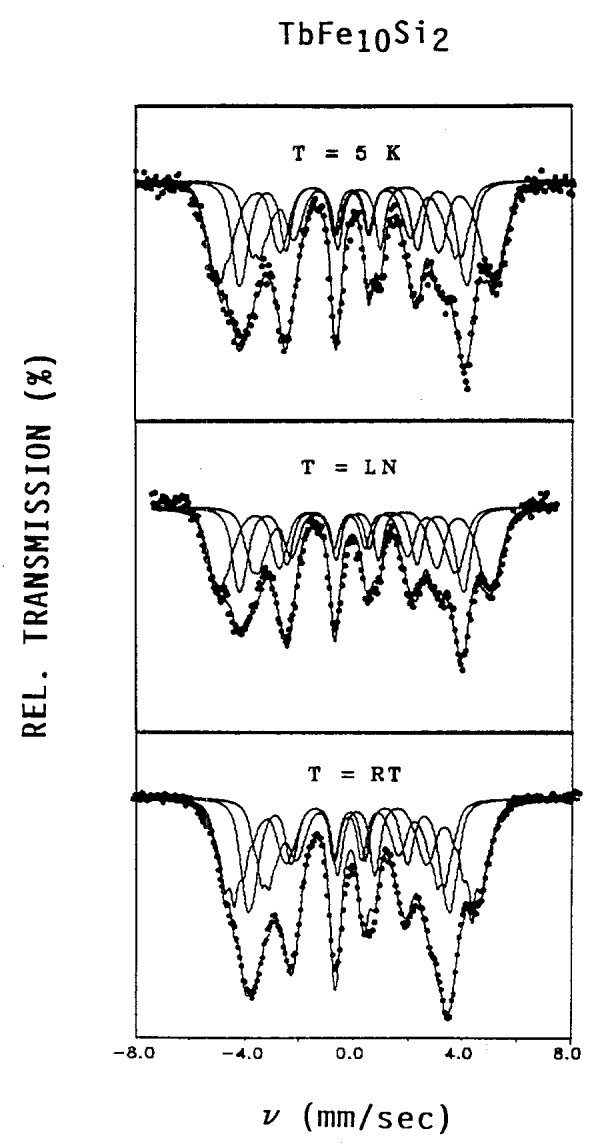

FIG. 6. Mössbauer spectra of $TbFe_{10}Si_2$ oriented absorbers.

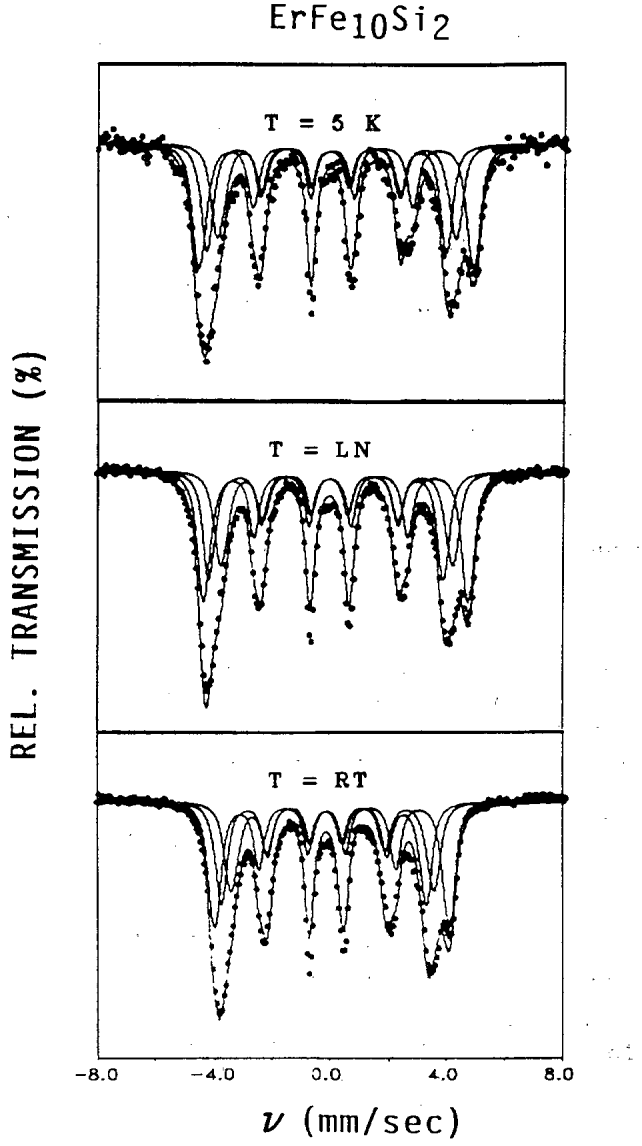

FIG. 7. Mössbauer spectra of $ErFe_{10}Si_2$ oriented absorbers.

TABLE I. Hyperfine parameters and relative absorptions x for the lines with $\Delta m_I=0$ in $R\mathrm{Fe}_{10}\mathrm{Si}_2$ compounds.

		B_{eff} (kG)			Δ_{IS} (mm/s)			Δ_{QS} (mm/s)			
R	$T(K)$	8i	8j	8f	8i	8j	8f	8i	8j	8f	x
Tb	5	307	225	256	0.149	0.033	−0.053	−0.046	0.020	0.020	1.6
	80	305	224	252	0.081	−0.058	−0.088	−0.050	0.104	−0.011	1.6
	300	279	196	226	0.046	−0.102	−0.155	−0.052	0.097	−0.007	1.3
Ho	5	293	257	258	0.118	0.125	−0.116	0.070	0.077	0.032	1.3
	80	186	247	252	0.116	0.114	−0.109	0.080	0.097	−0.057	1.3
	300	253	206	227	−0.008	−0.145	−0.092	0.073	0.078	−0.012	1.3
Er	5	292	252	254	0.126	0.114	−0.085	0.064	0.091	−0.061	1.3
	80	282	247	250	0.102	−0.110	0.087	0.085	0.102	−0.064	1.3
	300	250	216	259	−0.017	−0.233	−0.160	0.073	0.115	−0.069	1.4
Tm	5	293	258	258	0.111	0.130	−0.091	0.084	0.059	−0.040	1.3
	80	284	247	250	0.113	0.123	−0.100	0.078	0.071	−0.049	1.3
	300	250	209	223	−0.016	−0.094	−0.107	0.079	0.037	−0.001	1.3

at $T=290$ K, where the easy axis of magnetization is parallel to the c axis of the lattice, the spectrum is very similar to the spectra of Er, Ho, and Tm.

For R =Tb the Mössbauer spectra have shown fairly different shapes with broader absorption lines than the compounds with R =Er, Ho, or Tm. On the other hand, the Tb spectra are very similar to the spectra of $\mathrm{DyFe}_{10}\mathrm{Si}_2$, in the temperature range where the M_s makes an angle with the c axis. From the observed SRT in the thermomagnetic measurements (Figs. 2 and 3) of the Tb compound, it is obvious that there is an inclination of M_s from the c axis for temperatures $T<550$ K. This inclination causes an extra broadening in the distribution of the hyperfine fields.

In Table II we have tabulated the occupation probabilities p_{i}, p_{f}, and p_{j} which correspond to the best fits of the Mössbauer spectra at all temperatures for each compound. The normalization of these probabilities is chosen to give the nominal concentration $x=2$ of Si: $4p_{\mathrm{i}}+4p_{\mathrm{j}}+4p_{\mathrm{f}}=2$. The resulting preferential occupation of the 8j and 8f sites by Si, in contrast to the preference of the transition-metal elements T=Ti, and V for the 8i site,[4,5] is expected to cause different crystal-field interactions at the site of R^{3+} ions because of the different charge distribution in the vicinity of the R site and the metalloid character of Si atoms.

From the detailed temperature dependence of the relative intensities of Mössbauer spectra of $\mathrm{DyFe}_{10}\mathrm{Si}_2$, it is possible to calculate the tilting angle a of the M_s with respect to the c axis as shown in previous studies of $\mathrm{DyFe}_{11}\mathrm{Ti}$ and $\mathrm{NdFe}_{11}\mathrm{V}_2$,[7,8] to which we refer for the details of the calculation. The calculated values of a as a function of temperature are plotted in Fig. 8.

We conclude that the strength of Dy anisotropy at low temperatures is not large enough in order to rotate the magnetization in the (a,b) plane, perpendicular to the c axis. Also, the continuous and smooth variation of a in the wide temperature region 200–270 K is evidence of a second-order SRT transition.

TABLE II. Site occupation probabilities in $R\mathrm{Fe}_{10}\mathrm{Si}_{12}$ compounds.

R	p_{i}	p_{j}	p_{f}
Tb	0.00	0.25	0.25
Dy	0.04	0.21	0.25
Er	0.03	0.25	0.23
Ho	0.06	0.22	0.22
Tm	0.10	0.20	0.20

CEF CALCULATIONS FOR THE $R\mathrm{Fe}_{10}\mathrm{Si}_2$ and $R\mathrm{Fe}_{10}\mathrm{V}_2$ COMPOUNDS

The spin-reorientation data presented in the previous section can be used to derive the crystalline-electric-field coefficients for the studied compounds using the crystal-field and exchange interaction model, which has been applied successfully for the description of the magnetic properties of the $R_2\mathrm{Fe}_{14}\mathrm{B}$ compounds.[1] The details of this method have been described in the literature.[1,9] We

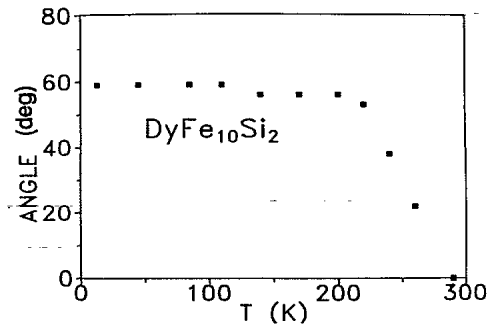

FIG. 8. Temperature dependence of the tilting angle a of $\mathrm{DyFe}_{10}\mathrm{Si}_2$ obtained from the analysis of Mössbauer spectra.

note only that the parameters entering in the calculation are the anisotropy constant K_1(Fe) for the iron sublattice, the mean-field coefficient $n_{R\mathrm{Fe}}$, and the CEF coefficients A_{nm}.

For the following calculations, the K_1(Fe) anisotropy energy parameters have been taken from $YFe_{10}V_2$ and $YFe_{10}Si_2$ compounds measured with the single-point detection (SPD) method as a function of temperature.[10] Values for the saturation magnetization M_s of Y compounds were derived from the high-field part of isotherm curves by extrapolation with the law of approach to saturation:

$$M=M_s(1-b/H^2+\cdots).$$

The iron sublattice anisotropy is uniaxial with, e.g., $K_1(\mathrm{Fe})\approx 1.7\times 10^7$ erg/cm^3 for $YFe_{10}V_2$ at 0 K.[10] Since the A_{20} coefficient of the rare earth is small, it is possible at higher temperatures for the Fe anisotropy to overcome the R anisotropy for the R^{3+} ions with $a_J<0$ and give rise to SRT.[2] The low values of A_{nm} can be attributed to the high symmetry ($4/mmm$) of the R lattice site in the 1:12 structure. As a starting point for the values of the CEF coefficients, we may take the set determined from magnetization measurements on a single crystal of $DyFe_{11}Ti$.[2] In a previous investigation of SRT,[3] we have shown that this set reproduces qualitatively the experimental results for the $RFe_{10}V_2$ series, but with significant discrepancies, notably in the case of the Nd and Dy compounds. In the latter case the calculation predicts two SRT, while subsequent ac susceptibility data[12] give evidence for only one transition. It is therefore plausible that this set of coefficients must be modified in order to correct these discrepancies. Since the site symmetry of the R ion is the same for all the compounds with the 1:12 structure, it is expected that the signs of the CEF parameters will not vary for different members of the series.

In view of these arguments, we have recalculated spin-reorientation temperatures for the $RFe_{10}V_2$ series using exactly the same signs for the A_{nm} as for $DyFe_{11}Ti$ and reducing the magnitudes by a common scaling factor. This choice is justified by the fact that V occupies preferentially the same sites as Ti, the main difference being in the increased V atomic content. A value of 0.69 for the scaling factor was found to give the best fit to the observed SRT. All the crystal-field terms B_{nm} and A_{nm}(V) at $T=0$ K are listed in Table III. For the description of the SRT in $HoFe_{10}V_2$, we have used 25% larger A_{40} and A_{44} terms relative to all the other V compounds. The variation of the angle a as a function of temperature resulting from these calculations is plotted in Fig. 9, and a comparison between the experimental and calculated T_{SR} is given in Table IV. For the case of $TbFe_{10}V_2$, this crystal-field model fails because of the possible mixing of the valence states +3 and +4 of the Tb ion. However, the agreement between T_{SR}(expt) and T_{SR}(calc) is very good for all the other compounds. The SRT for the compounds with $R=Nd^{3+}$, and Ho^{3+} are first-order transitions, while for the rest are of second order. Characteristic is the absence of the first-order transition which was predicted earlier for $DyFe_{10}V_2$,[3] but is not observed experimentally.[12]

In the $RFe_{10}Si_2$ series, the significant change of the charge configuration in the vicinity of the R^{3+} ion as a consequence of the different preferential site occupation and electronic configuration of the Si atoms makes more complicated the estimation of A_{nm}(Si) than the A_{nm}(V). Hence the calculated A_{nm}(Si) values are not related to those of Ti or V compounds with a unique scaling factor. In this series of compounds, SRT transitions are observed

TABLE III. Crystal-field parameters at $T=0$ K. B_{nm} in K/ion and crystalline-electric-field coefficients A_{nm} in K/a_0^{-n} for $RFe_{10}T_2$ (T=V or Si) compounds.

R^{3+}	Nd^{3+}	Dy^{3+}	Ho^{3+}	Er^{3+}	Tm^{3+}
			T=V		
10^2B_{20}	16.0	11.0	4.0	4.0	15.0
10^4B_{40}	72.5	7.6	5.2	−4.8	−16.4
10^4B_{44}	−690	−72.5	−49.8	45.9	156
10^6B_{60}	−1007	11.5	−12.3	17.6	−42.9
10^6B_{64}	−252	2.7	−3.1	4.4	−10.7
	A_{20}	A_{40}	A_{44}	A_{60}	A_{64}
	−22.3	−8.5[a]	81.4[a]	1.77	0.44
			T=Si		
R^{3+}	Tb^{3+}	Dy^{3+}	Ho^{3+}	Er^{3+}	Tm^{3+}
10^2B_{20}	51.1	30.5	10.2	−11.1	−42.3
10^4B_{40}	−28.3	12.5	6.4	−7.9	−26.8
10^6B_{44}	−7.7	6.2	−23.2	9.9	−24.2
10^6B_{60}	−2.6	2.1	−7.8	3.3	−8.2
	A_{20}	A_{40}	A_{44}	A_{60}	A_{64}
	−61.6	−14.0	8.3	1.0[b]	0.3[b]

[a]For $HoFe_{10}V_2$, $A_{40}=-11.4$, and $A_{44}=108.5Ka_0^{-4}$.
[b]For $HoFe_{10}Si_2$, $A_{60}=3.3$, and $A_{64}=1.1Ka_0^{-6}$.

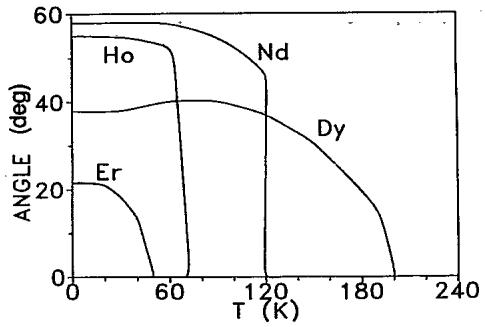

FIG. 9. Calculated temperature dependence of the tilting angle a for the $R\mathrm{Fe}_{10}\mathrm{V}_2$ compounds.

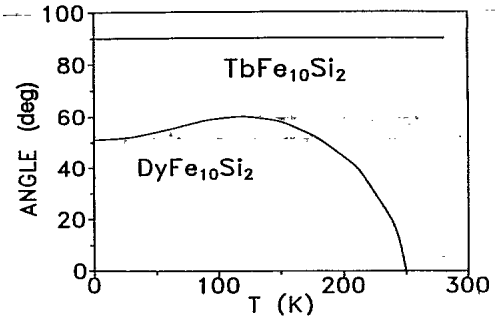

FIG. 10. Calculated temperature dependence of the tilting angle a for the $R\mathrm{Fe}_{10}\mathrm{Si}_2$ compounds.

in the Dy member at ≈ 260 K and the Tb member at ≈ 550 K, while the Er and Tm compounds have easy-axis anisotropy, as expected from the signs of a_J and A_{20}.

A consistent set of crystal-field coefficients should reproduce the observed variation of tilting angle a for $\mathrm{DyFe}_{10}\mathrm{Si}_2$ (Fig. 8) and the anisotropy properties of the other compounds. In Table III are listed all the crystal-field terms at $T=0$ K which give the best agreement with the experimental data. The variation of the angle a with temperature is plotted in Fig. 10 for $R=$Dy and Tb. The angle for Tb remains at 90° up to above 300 K, in disagreement with the experimental results, which indicate a first-order transition at ≈ 550 K, and subsequent continuous rotation of the M_s, which seems to reach a stable inclination angle a at ≈ 170 K. As has been noted, however, a discrepancy between calculated and experimental results for Tb is found also in the Ti (Ref. 2) and V (Ref. 3) series and has been attributed to admixture of the Tb^{4+} state.

A modification of the CEF coefficients given in Table III was also found necessary for the $\mathrm{HoFe}_{10}\mathrm{Si}_2$ compound. Here the sixth-order coefficients are increased by a factor of 1.7 to explain the absence of a SRT. This should be contrasted to the behavior of the $\mathrm{HoFe}_{10}\mathrm{V}_2$ compound, where a SRT is observed,[3] while no SRT is found in $\mathrm{HoFe}_{11}\mathrm{Ti}$. These results give further evidence for the delicate balance of crystal-field anisotropy of different orders that exists in the Ho compounds. For $\mathrm{ErFe}_{10}\mathrm{Si}_2$ and $\mathrm{TmFe}_{10}\mathrm{Si}_2$, the coefficients of Table III predict correctly easy-axis anisotropy at all temperatures.

TABLE IV. A comparison of the observed $T_{\mathrm{SR}}^{\mathrm{expt}}$ and calculated $T_{\mathrm{SR}}^{\mathrm{calc}}$ SRT temperatures, mean-field exchange coefficients $n_{R\mathrm{Fe}}$, and Curie temperatures T_C for the $R\mathrm{Fe}_{10}\mathrm{V}_2$ compounds.

$R\mathrm{Fe}_{10}\mathrm{V}_2$	T_C (K)	$n_{R\mathrm{Fe}}$ (μ_0)	$T_{\mathrm{SR}}^{\mathrm{expt}}$ (K)	$T_{\mathrm{SR}}^{\mathrm{calc}}$ (K)
Nd	570	325	120	120
Tb	570	184	170	
Dy	540	175	200	200
Ho	525	196	60	65
Er	505	170	65	50

DISCUSSION

The results presented in the previous section help to enrich and extend our understanding of the crystal-field interactions in the 1:12 rare-earth iron intermetallic compounds. The main feature that emerges, confirming previous investigations, is the small value of the second-order crystal-field coefficients and hence the importance of higher-order terms. The values of A_{20} are found in the range of $-20Ka_0^{-2}$ ($R\mathrm{Fe}_{10}\mathrm{V}_2$) to $-60Ka_0^{-2}$ ($R\mathrm{Fe}_{10}\mathrm{Si}_2$), which can be contrasted to the value of $\approx 300Ka_0^{-2}$ for the $R_2\mathrm{Fe}_{14}B$ compounds. Another feature of interest is the existence of a great variety of compounds with the same crystal structure, but with sufficiently different elemental and electronic composition to allow potentially greater variations in the values of A_{nm} than, e.g., in the $R_2\mathrm{Fe}_{14}\mathrm{B}$ series. We shall make some remarks that arise from these features from an overview of our and previous investigations.

The nature of the observed transitions can be discussed with reference to the relations[13] which give the anisotropy constant for the rare-earth ion. From these relations it is seen that to a first approximation the negative value of A_{20} favors planar orientation for the $a_J<0$ ions (Nd^{3+}, Tb^{3+}, Dy^{3+}, and Ho^{3+}) and easy-axis orientation for the $a_J>0$ ions (Sm^{3+}, Er^{3+}, and Tm^{3+}). However, when A_{20} is of comparable magnitude with higher-order terms, SRT may occur at low temperatures where the expectation values of all the $\langle O_{nm}\rangle$ are important. In the case of $\mathrm{DyFe}_{10}\mathrm{Si}_2$, for example, the second-order term $B_{20}\langle O_{20}\rangle$ is much smaller than the higher-order terms and the variation of tilting angle with temperature up to the SRT is very sensitive to the value of the sixth-order term. More generally, the importance of the sixth-order term must be emphasized for the occurrence of SRT at low temperatures in all 1:12 compounds. The effect of this term causes the unexpected SRT in $\mathrm{ErFe}_{11}\mathrm{Ti}$ (Ref. 2) and $\mathrm{ErFe}_{10}\mathrm{V}_2$ (Ref. 3) compounds. The relatively higher second- and fourth-order terms in combination with the lower sixth-order term are necessary to predict the absence of a SRT in $\mathrm{ErFe}_{10}\mathrm{Si}_2$.

The results presented here demonstrate that the SRT in the $R\mathrm{Fe}_{12-x}T_x$ series cannot be reproduced with nearly the same set of A_{nm} coefficients when T varies. For the same T and x, this is possible with the notable excep-

TABLE V. Listing of A_{n0} crystalline-electric-field coefficients for the three $R\mathrm{Fe}_{12-x}T_x$ alloys with T=Ti, V, and Si as a function of concentration x and preferential site occupation of T atoms.

$R\mathrm{Fe}_{12-x}T_x$	x	Site	A_{20}	A_{40} (Ka_0^{-n})	A_{60}
T=Ti	1	8i	−32.3	−12.4	2.56
V	2	8i	−22.3	−8.5	1.77
Si	2	8j,8f	−61.6	−14.0	1.00

tion of the Ho compounds. Our values of A_{20} are significantly smaller than the values derived from ^{155}Gd Mössbauer studies of $GdFe_{10}V_2$ and $GdFe_{10}Si_2$.[6] Other Mössbauer data, however, for $GdFe_{11}Ti$ give a value of $A_{20}=-30Ka_0^{-2}$.[2]

The choice of larger values for the higher-order coefficients A_{nm} ($n\geq 4$), which have been used exceptionally for Ho compounds in the V and Si series for the reproduction of the SRT of these alloys, at first sight may appear arbitrary. This, however, was the result of an extensive search in parameter space, in which it was found impossible to reproduce the experimental data for *all* compounds with the same A_{nm} coefficients. This remark applies also more generally to the uniqueness of the sets of coefficients derived in the present work. Although it is difficult to assign errors by a fitting procedure, our calculations indicate that a deviation of more than 10% from the given values causes serious disagreement between experimental and calculated results. In the case of the 1:12 compounds with T=V and Si, the Ho alloys present a deviation of the higher-order terms A_{4m} and A_{6m}, respectively, which seems to be related with the delicate balance between the different contributions to anisotropy. Since the higher-order crystalline-electric-field coefficients are determined mainly from intra-atomic Coulomb and exchange interactions between $4f$-$5d$ and $6s$-$6p$ shells, the A_{4m} and A_{6m} terms are not expected to remain constant across the R series in isomorphic structures.

A comparison of the resulting A_{nm} from this model of CEF calculations for the three different series $R\mathrm{Fe}_{11}\mathrm{Ti}$, $R\mathrm{Fe}_{10}\mathrm{V}_2$, and $R\mathrm{Fe}_{10}\mathrm{Si}_2$ is given in Table V in which we have also included the site occupation of the T element. Although the data are limited, a correlation may be suggested between the occupation of the 8i site and the strength of the crystal field as expressed by the absolute values of A_{n0} coefficients, which seems to decrease systematically with the increased substitution of T elements. It can be noted in this connection that the 8i site has the shortest distance to the rare-earth ion so that variations in its occupancy may have greater effect on the electric field at the rare-earth site.

CONCLUSIONS

With the additional experimental results on the magnetic structures of the series $R\mathrm{Fe}_{10}\mathrm{Si}_2$ (R =Tb, Dy, Ho, Er, or Tm), which form part of the large class of the pseudobinary intermetallic compounds of the type $R\mathrm{Fe}_{12-x}T_x$, we have now an extensive set of data on which our understanding of crystal-field and exchange interactions can be tested. The model for the calculation of magnetic structure which was developed for the $R_2\mathrm{Fe}_{14}\mathrm{B}$ series has been applied to a much wider class of compounds of the same crystal structure, but with strong differences in elemental and electronic composition. With the exception of a few cases, the observed magnetic transitions can be successfully described and the following facts may be considered as established.

(a) The second-order crystal-field coefficients A_{20} are negative, but not dominant. Fourth- and sixth-order terms play a decisive role in determining SRT.

(b) The set of crystal-field coefficients depends on the type of the element T and, to a lesser extent, on the concentration x.

ACKNOWLEDGMENTS

This work was supported in part by an E.E.C. Contract No. MA-1E-0052 in the framework of the BRITE-EURAM program.

*Present address: Trinity College, Physics Department, Dublin 2, Ireland.

[1]J. M. D. Coey, Hong-Shuo Li, J. P. Gavigan, J. M. Gadogan, and Bo-Ping Hu, *The Concerted European Action on Magnets* (Elsevier, London, 1989), p. 76.

[2]Bo-Ping Hu, Hong-Shuo Li, J. M. D. Coey, and J. P. Gavigan, Phys. Rev. B **41**, 2221 (1990).

[3]C. Christides, D. Niarchos, A. Kostikas, Hong-Shuo Li, Bo-Ping Hu, and J. M. D. Coey, Solid State Commun. **72**, 839 (1989).

[4]R. B. Helmhold, J. J. M. Vleggaar, and K. H. J. Buschow, J. Less-Common Met. **144**, 209 (1988).

[5]O. Moze, L. Pareti, M. Solzi, and W. I. F. David, Solid State Commun. **66**, 465 (1988).

[6]K. H. J. Buschow, D. B. De Mooij, M. Brouha, H. H. A. Smit, and R. C. Theil, IEEE Trans. Magn. **MAG-24**, 1161 (1988).

[7]C. Christides, A. Kostikas, A. Simopoulos, D. Niarchos, and G. Zouganelis, J. Magn. Magn. Mater. **86**, 367 (1990).

[8]Hong-Shuo Li, Bo-Ping Hu, and J. M. D. Coey, Solid State Commun. **66**, 133 (1988).

[9]M. Cadogan, J. P. Gavigan, D. Givord, and Hong-Shuo Li, J. Phys. F **18**, 779 (1988).

[10]M. Solzi, L. Pareti, O. Moze, and W. I. F. David, J. Appl. Phys. **64**, 5084 (1988).

[11]F. R. de Boer, Huang Ying-Kai, D. B. de Mooij, and K. H. J. Buschow, J. Less-Common. Met. **135**, 199 (1987).

[12]P. A. Algarabel and M. R. Ibarra, Solid State Commun. **74**, 231 (1990).

[13]C. Rudowicz, J. Phys. C **18**, 1415 (1985).